

---

# Autobahn: Automorphism-based Graph Neural Nets

---

**Erik H. Thiede**

Center for Computational Mathematics  
Flatiron Institute  
New York, NY 10010  
ehthiede@flatironinstitute.org

**Wenda Zhou**

Center for Data Science  
New York University  
New York, NY 10011  
wz2247@nyu.edu

**Risi Kondor**

Department of Computer Science and Department of Statistics  
University of Chicago  
Chicago, IL 60637  
risi@uchicago.edu

## Abstract

We introduce Automorphism-based graph neural networks (Autobahn), a new family of graph neural networks. In an Autobahn, we decompose the graph into a collection of subgraphs and apply local convolutions that are equivariant to each subgraph’s automorphism group. Specific choices of local neighborhoods and subgraphs recover existing architectures such as message passing neural networks. Our formalism also encompasses novel architectures: as an example, we introduce a graph neural network that decomposes the graph into paths and cycles. The resulting convolutions reflect the natural way that parts of the graph can transform, preserving the intuitive meaning of convolution without sacrificing global permutation equivariance. We validate our approach by applying Autobahn to molecular graphs, where it achieves state-of-the-art results.

## 1 Introduction

The successes of artificial neural networks in domains such as computer vision and natural language processing have inspired substantial interest in developing neural architectures on graphs. Since graphs naturally capture relational information, graph-structured data appears in a myriad of fields. However, working with graph data raises new problems. Chief among them is the problem of graph isomorphism: for the output of our neural network to be reliable, it is critical that the network gives the same result independent of trivial changes in graph representation such as permutation of nodes.

Considerable effort has gone into constructing neural network architectures that obey this constraint 6, 13, 21, 31, 33. Arguably, the most popular approach is to construct *Message-Passing Neural Networks (MPNNs)* 18, 24. In each layer of an MPNN, every node aggregates the activations of its neighbors in a permutation invariant manner and applies a linear mixing and nonlinearity to the resulting vector. While subsequent architectures have built on this paradigm, e.g., by improving activations on nodes and graph edges 22, 35, the core paradigm of repeatedly pooling information from neighboring nodes has remained. These architectures are memory efficient, intuitively appealing, and respect the graph’s symmetry under permutation of its nodes. However, practical results have shown that they can oversmooth signals 27 and theoretical work has shown that they have trouble distinguishing certain graphs and counting substructures 2, 8, 17, 35. Moreover, MPNNs do not use the graph’s topology to its fullest extent. For instance, applying an MPNN to highly structured graphs such as grid graphs does not recover powerful known architectures such as convolutional neural networks. It is also not clear how to best adapt MPNNs to families of graphs with radically different

topologies: MPNNs for citation graphs and molecular graphs are constructed in largely the same way. This suggests that it should be possible to construct more expressive graph neural networks by directly leveraging the graph’s structure.

In this work, we introduce a new framework for constructing graph neural networks, *Automorphism-based Neural Networks* (Autobahn). Our research is motivated by our goal of designing neural networks that can learn the properties of small organic molecules accurately enough to make a significant contribution to drug discovery and materials design 4, 19, 26, 32. The properties of these molecules depend crucially on multi-atom substructures, making the difficulties MPNNs have in recognizing substructures a critical problem. We realized that we could circumvent this limitation by making graph substructures *themselves* the fundamental units of computation. The symmetries of our substructures then inform the computation. For instance, the benzene molecule forms a ring of 6 atoms and is a common subunit in larger molecules. On this ring we have very natural and mathematically rigorous notion of convolution: convolution on one-dimensional, periodic domain. This symmetry is encoded by a graph’s automorphism group: the group that reflects our substructures’ internal symmetries. Our networks directly leverage the automorphism group of subgraphs to construct flexible, efficient neurons. Message passing neural networks arise naturally in this framework when the substructures used are local star graphs, and applying Autobahn to grid graphs can recover standard convolutional architectures such as steerable CNNs. More generally, Autobahn gives practitioners the tools to build bespoke graph neural networks whose substructures reflect their domain knowledge. As an example, in Section 6, we present a novel architecture outside of the message-passing paradigm that nevertheless achieves state of the art performance on molecular learning tasks.

## 2 Graph Neural Networks

Neural Networks operate by composing several learned mappings known as “layers”. Denoting the  $\ell$ ’th layer in the network as  $\phi_\ell$ , the functional form of a neural network  $\Phi$  can be written as

$$\Phi = \phi_L \circ \phi_{L-1} \circ \dots \circ \phi_1.$$

Each layer is typically constructed from a collection of parts, the titular “neurons”. We denote the  $i$ ’th neuron in the  $\ell$ ’th layer as  $n_i^\ell$ , and denote its output (the “activation” of the neuron) as  $f_i^\ell$ . Architectures differ primarily in how the neurons are constructed and how their inputs and outputs are combined.

When constructing a neural network that operates on graph data, care must be taken to preserve input graphs’ natural symmetries under permutation. Let  $\mathcal{G}$  be a graph with node set  $\{v_1, \dots, v_n\}$ , adjacency matrix  $A \in \mathbb{R}^{n \times n}$  and  $d$ -dimensional node labels  $b_i \in \mathbb{R}^d$  stacked into a matrix  $B \in \mathbb{R}^{n \times d}$ . Permuting the numbering of the nodes of  $\mathcal{G}$  by some permutation  $\sigma: \{1, 2, \dots, n\} \rightarrow \{1, 2, \dots, n\}$  transforms:

$$A \mapsto A^\sigma \quad A_{i,j}^\sigma = A_{\sigma^{-1}(i), \sigma^{-1}(j)}, \quad (1)$$

and

$$B \mapsto B^\sigma \quad B_{i,n}^\sigma = B_{\sigma^{-1}(i), n}. \quad (2)$$

This transformation does not change the actual topology of  $\mathcal{G}$ . Consequently, a fundamental requirement on graph neural networks is that they be invariant with respect to such permutations.

### 2.1 Message-Passing Neural Networks

Message-passing neural networks (MPNNs) have emerged as the dominant paradigm for constructing neural networks on graphs. Every neuron in an MPNN corresponds to a single node in the graph. Neurons aggregate features from neighboring nodes by passing them through a function that is invariant to permutation of its inputs. They then combine the result with the node’s original message, and pass the result through a learned linear function and nonlinearity (Figure 1) 35. Since information is transmitted over the graph’s topology, MPNNs are not confounded by permutations of the graph. Many variations on this scheme have been proposed in the literature. Specific architectures may differ in the details of the aggregation function 15, 20, 24, 35, may include additional terms to account for edge features 22, 35, may use complex transformations to construct the node features encoding local structure 1, 5, or may augment the graph with additional nodes 16, 23.

## 3 Permutation Equivariance

As discussed in the Introduction, MPNNs have fundamental limits to their expressiveness. To construct more powerful neural networks, we turn to the general formalism of group equivariant

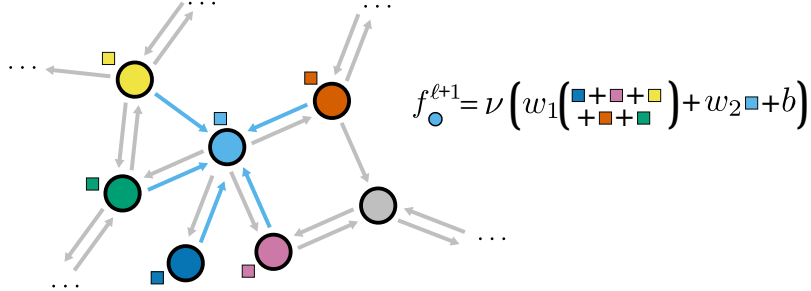


Figure 1: Visualization of a single layer of a simple message passing neural network. Each node aggregates the features from neighboring nodes using a permutation-invariant operation (we use summation for simplicity), applies learned weight matrices and biases and finally a nonlinearity.

networks 9–11, 25. Our desire that permutations of the input graph leave our network’s output unaffected is formalized by the notion of group-invariance. Let our input data live in a space  $X$  that is acted on by a group  $G$ , and for all  $g \in G$  denote the associated group action on  $X$  by  $T_g$ . The invariance constraint amounts to requiring:

$$\Phi = \Phi \circ T_g \quad \forall g \in G. \quad (3)$$

One way to accomplish this would be to require that each layer  $\phi_\ell$  be fully invariant to  $G$ . However, in practice this condition can be extremely restrictive. For this reason, networks commonly use group *equivariant* layers. Let  $X$  and  $Y$  be the input and output spaces of  $\phi_\ell$ , with group actions  $T_g$  and  $T'_g$ , respectively. We say  $\phi_\ell$  is equivariant to  $G$  if it obeys

$$T'_g \circ \phi_\ell = \phi_\ell \circ T_g \quad \forall g \in G. \quad (4)$$

This condition is weaker than invariance: we recover invariance when  $T'_g$  maps every element of  $Y$  to itself. Moreover, it is simple to show that the composition of two equivariant layers is also equivariant. Consequently, in all layers but the last we can enforce the weaker condition of equivariance and merely enforce invariance in the final layer. In the case of graph neural networks, the relevant group is the group of permutations:  $\mathbb{S}_n$  (called the symmetric group).

### 3.1 Permutation-equivariant networks

Recent work has developed a generic recipe for constructing group equivariant networks. In this formalism, any object that transforms under a group action is treated as a function on the group 25 (see Section 1 in the supplement for a brief review). This allows all objects equivariant to the group to be treated using the same formalism, independently of their particular transformation properties. In particular, it can be shown that the only group-equivariant linear operation possible is a generalized notion of convolution with respect to the group structure. For discrete groups, this convolution can be written as:

$$(f * w)(u) = \sum_{v \in G} f(uv^{-1})w(v). \quad (5)$$

To construct an equivariant neuron, we apply (5) to convolve our input activation  $f^{\ell-1}$  with a learned weight function  $w$ , add a bias and then apply a fixed equivariant nonlinearity,  $\nu$ . Applying this approach to specific groups recovers the standard convolutional layers used in convolutional neural networks (CNNs). For instance, applying (5) to the cyclic group of order  $n$  gives

$$(f * w)_j = \sum_{r=0}^n f(r^{j-k})w(r^k), \quad (6)$$

where  $r$  is the group element corresponding to rotation by  $360/n$  degrees. Similarly, applying (5) to one-dimensional or two-dimensional discrete translation groups recovers the standard convolutions used for image processing.

Instantiating this theory with the symmetric group has been successfully used to construct permutation equivariant networks for learning sets 36 and graph neural networks 28–30, 34. However, enforcing equivariance to all permutations can be very restrictive. As an example, consider a layer whose domain and range transform according to (2) with  $c_{in}$  incoming and  $c_{out}$  outgoing channels. Let

---

**Algorithm 1** Automorphism-based Neuron

---

**Input:**
 $f^{\ell-1}$  ▷ Incoming activation associated with  $\mathcal{G}$   
 $A_{\mathcal{G}}$  ▷ Adjacency matrix of  $\mathcal{G}$   
 $A_{\mathcal{T}}$  ▷ Adjacency matrix of the saved template graph.

- 1: Find  $\mu \in \mathbb{S}_n$  such that  $A_{\mathcal{G}}^{(\mu)} = A_{\mathcal{T}}$ .
- 2:  $(f^{\ell-1})^{(\mu)} \leftarrow T_{\mu}(f^{\ell-1})$  ▷ Apply  $\mu$  to incoming activation.
- 3:  $(f^{\ell})^{(\mu)} \leftarrow \nu((f^{\ell-1})^{(\mu)} * w + b)$  ▷ Convolution is over  $\text{Aut}(\mathcal{T})$ .
- 4:  $f^{\ell} \leftarrow T'_{\mu^{-1}}((f^{\ell})^{(\mu)})$  ▷ Map output to original ordering

**Return:**  $f^{\ell}$ 


---

$w_1, w_2 \in \mathbb{R}^{c_{out} \times c_{in}}$  be learned weight matrices, and  $f_j \in \mathbb{R}^{c_{in}}$  be the vector of incoming activations corresponding to node  $j$ . Under these conditions, the most general possible convolution is given by 36:

$$(f * w)_i = w_1 f_i + w_2 \sum_{j=1}^n f_j, \quad (7)$$

but this is quite a weak model because it only has two parameters and activations from different nodes only interact through their sum. Consequently, specific relationships between individual nodes are immediately lost. One possible approach that has been investigated in the literature is to consider higher order activations carrying information about pairs and triplets of nodes 29, 34. However, the Fourier structure of the symmetric group implies that the cost of even storing the activations scales as  $n^2, n^3$ , or higher, making them impractical to use for all but the smallest graphs. In particular, representing a 6-node structure such as a benzene ring would require sixth order activations ( $n^6$ ), which is completely infeasible.

## 4 Permutation-Equivariant Neurons using Automorphism

The key theoretical idea underlying our work is that to construct more flexible neural networks, we can exploit the graph topology itself. In particular, the local adjacency matrix itself can be used to judiciously break permutation symmetry, allowing us to identify nodes up to the symmetries of  $A$ . Letting  $\mathcal{G}$  be a graph as before, the automorphism group  $\text{Aut}(\mathcal{G})$  is:

$$\text{Aut}(\mathcal{G}) = \{\sigma \in \mathbb{S}_n | A^{\sigma} = A\}, \quad (8)$$

where  $A^{\sigma}$  is defined as in (1). Figure 2a shows the automorphism group of three example graphs.

If  $\mathcal{G}$  and  $\mathcal{G}'$  are two isomorphic graphs, then each node or edge in  $\mathcal{G}'$  can always be matched to a node or edge in  $\mathcal{G}$  up to a permutation in  $\text{Aut}(\mathcal{G})$ . If every graph our network observed was in the same isomorphism class, we could construct a neuron in a permutation-equivariant neural network by matching  $\mathcal{G}$  to a template graph  $\mathcal{T}$  and convolving over  $\text{Aut}(\mathcal{T})$ . We give pseudocode for such a neuron, which we call an ‘‘Automorphism-based neuron,’’ in Algorithm 1. Note that although the convolution itself is only equivariant to  $\text{Aut}(\mathcal{T})$ , the entire neuron is permutation-equivariant. A formal proof of equivariance is given in Section 2 of the Supplement.

For a given input and output space, neurons constructed using Algorithm 1 are more flexible than a neuron constructed using only  $\mathbb{S}_n$  convolution. As an example, consider a neuron operating on graphs isomorphic to the top left graph in Figure 2a and whose input and output features are a single channel of node features. An  $\mathbb{S}_n$ -convolution would operate according to (7): Each output node feature would see only the corresponding input feature and an aggregate of all other node features. In contrast, Algorithm 1 completely canonicalizes the graph since it has no non-trivial automorphism. Consequently, we do not need to worry about enforcing symmetry and we can simply run a fully connected layer: a richer representation. Similarly, Figure 2b depicts an analogous neuron constructed in the presence of cyclic graph symmetry. In this case, the matching can be performed up to a cyclic permutation, so convolution must be equivariant to the graph’s automorphism group  $C_6$ .

This strategy was first discussed in 12. While the increased flexibility was noted, the authors also observed rightfully that this strategy is not directly practical. Most graph learning problems consist either of many graphs from different isomorphism classes or a single large graph that is only partially known. In the former case, we would have to construct one network for every isomorphism class

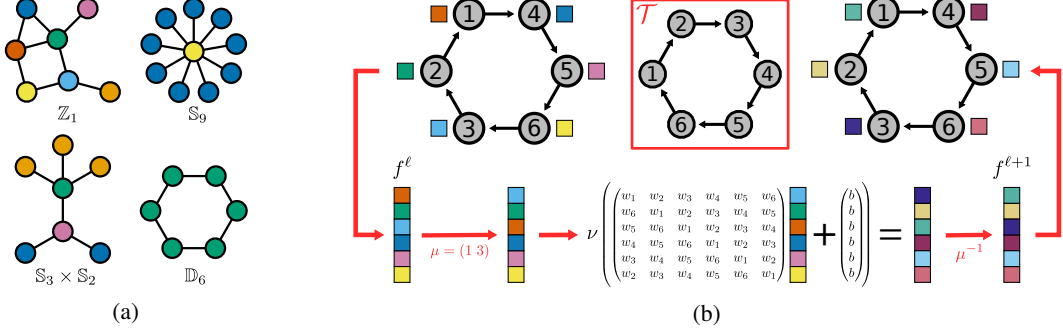


Figure 2: Figures visualizing the automorphism group of a graph and its use in graph learning. (a) Four graphs and their automorphism groups. In each graph, nodes in the same orbit of the graph’s automorphism group are the same color. (b) An neuron constructed by applying Algorithm 1 to a cyclic directed graph. We consider the simplified setting where the layer operates only on a single channel of node features. Note that the matching step can only be accomplished up to an element in the graph’s automorphism group: the cyclic group of order 6,  $\mathbb{C}_6$ .

and each network would only see a fraction of the data. In the latter, the isomorphism class of the network would be unknown. Indeed, the architecture ultimately proposed in 12, local natural graph networks, did not explicitly use convolutions against the automorphism group but instead combined multiple message passing networks, each applied to a local neighborhood of the graph.

## 5 Autobahn

To motivate our approach we consider MPNNs from the perspective of Algorithm 1. Looking at Figure 1 we see that the message-passing procedure itself forms a star graph, where the leaves of the star correspond to the neighboring nodes. The automorphism group of a star graph is the set of all permutations that swap the star’s leaves. This is precisely the group structure of a single MPNN neuron. Since we apply a permutation-invariant aggregation function, if we were to permute a neuron’s input data between the leaves of the star, the MPNN neuron would be unaffected. However, permuting the input features for the central node with one of its neighbors could “break” the MPNN.

This suggests a natural generalization of MPNNs. In every layer, we decompose a graph into a collection of subgraphs known as “local graphs” that are isomorphic to a pre-selected template graph.<sup>1</sup> Every local graph corresponds to a permutation-equivariant neuron; we denote the local graph of neuron  $n_j^\ell$  as  $\mathcal{G}_j^\ell$ . Each neuron operates by aggregating information from overlapping local graphs and then applying Algorithm 1 to the result. Because of the important role played by convolutions over subgraphs’ automorphism groups, we refer to the resulting networks as Autobahn-based Neural Networks, or Autobahns.

By using star-graph shaped templates, the Autobahn formalism can recover MPNNs. However, these are not the only commonly used algorithm that can be recovered by the Autobahn formalism. In Section 3 in the supplement we show that using a grid graph template on a larger grid graph recovers steerable CNNs 10.<sup>2</sup> The fact that Autobahn networks naturally recover these architectures when MPNNs do not suggests that considering the local automorphism group is a productive direction for incorporating graph structure.

In the discussion that follows, we give a generic treatment of each step in the network, followed by a full description of an Autobahn layer. We do not specify a specific form for the activations: they may correspond to individual nodes, edges, hyper-edges, or be delocalized over the entire local graph as in. This is in keeping with our philosophy of giving a flexible recipe that practitioners can tailor to their specific problems using their domain knowledge.

<sup>1</sup>This requires solving a subgraph isomorphism problem. While this is can be hard for pathological families of  $\mathcal{G}$  or template graphs, for “real world” graphs we expect that it can be solved efficiently.

<sup>2</sup>Standard CNNs further break the symmetry of the grid graph by introducing a notion of up/down and left/right. However, if we introduce a notion of edge “color” to distinguish horizontal from vertical edges and extend our definition of automorphism to include color, Autobahn can recover CNNs as well: see Section 3 in the Supplement.

## 5.1 Convolutions using the Automorphism Group

The convolutions in Autobahn proceed by applying Algorithm 1 to each neuron’s local graph. The precise form of the convolution will depend on how the activation transforms under permutation. In 25 it was observed that for any compact group, one could construct a group convolution by transforming an activation into the group’s Fourier space and using the convolution theorem. That said, for specific groups simple convolutions are either known or intuitive to derive. For instance, in Section 6 our architecture uses directed cycle and path graphs as templates. There, group convolutions can be performed using well-known one-dimensional convolutions such as (6).

## 5.2 Transferring information across neurons

To build a rich representation of the structure graph we must be able to transmit information between neurons operating on different local graphs. In MPNNs and CNNs, each neuron pools information into the central node before transmitting to its neighbors. This simplifies the task of transmitting information to other neurons, as the output of neuron  $n_j^\ell$  becomes a node feature for neuron  $n_k^{\ell+1}$ . However, this strategy does not necessarily work for the neurons in Autobahn: our local graphs may not have a central node. Even if they do, collapsing each neuron’s output into a single node limits our networks expressivity, as it prevents neurons from transmitting equivariant information such as the hidden representations of multiple nodes or (hyper)edges.

Instead, we observe that any part of an activation that corresponds to nodes shared between two local graphs can be freely copied between the associated neurons. To transmit information from  $n_j^{\ell-1}$  to  $n_j^\ell$ , we define two operations, narrowing and promotion, that extend this copying procedure to arbitrary activations. Narrowing compresses the output of  $n_j^{\ell-1}$  into the intersection of the two local graphs, and promotion expands the result to the local graph of  $n_j^\ell$ .

To ensure that narrowing and promotion are defined for all activations regardless of their specific group actions, we employ the formalism from 25 where activations are treated as functions on the symmetric group. Specifically, the input activation and narrowed activation are identified with functions from  $\mathbb{S}_m$  to  $\mathbb{R}$  and  $\mathbb{S}_k$  to  $\mathbb{R}$ , respectively. We discuss special cases after the definitions, and depict a specific example operating on edge features in Figure 3.

### 5.2.1 Narrowing

Narrowing takes an activation  $f$  that transforms under permutation of a given set of  $m$  nodes and converts it into a function that transforms only with respect to a subset of  $k < m$  nodes,  $\{v_{i_1}, \dots, v_{i_k}\}$ . To construct our narrowed function, we apply an arbitrary permutation that “picks out” the nodes  $\{i_1, \dots, i_k\}$  by sending them to the first  $k$  positions. (Note this implicitly orders these nodes.) Subsequent permutations of  $\{1, 2, \dots, k\}$  permutes our specially chosen nodes amongst each other and permutations of  $\{k+1, \dots, m\}$  permutes the other, less desirable nodes. Narrowing exploits this to construct a function on  $\mathbb{S}_k$ : we apply the corresponding group element in  $\mathbb{S}_k$  to the first  $k$  positions, average over all permutations of the last  $m-k$ , and read off the result.

**Definition 1.** Let  $(i_1, \dots, i_k)$  be an ordered subset of  $\{1, 2, \dots, m\}$  and  $t$  be an (arbitrarily chosen) permutation such that

$$t(i_p) = p \quad \forall p \in 1, \dots, k. \quad (9)$$

For all  $u \in \mathbb{S}_k$  let  $\hat{u} \in \mathbb{S}_m$  be the permutation in that applies  $u$  to the first  $k$  elements and for all  $s \in \mathbb{S}_{m-k}$  let  $\hat{s} \in \mathbb{S}_m$  be the permutation that applies  $s$  to the last  $m-k$  elements. Given  $f: \mathbb{S}_m \rightarrow \mathbb{R}^d$  we define the **narrowing** of  $f$  to  $(i_1, \dots, i_k)$  as the function:

$$f \downarrow_{(i_1 \dots i_k)}(u) = (n-k)!^{-1} \sum_{s \in \mathbb{S}_{m-k}} f(\hat{u} \hat{s} t). \quad (10)$$

Narrowing obeys a notion of equivariance for permutations restricted to the local graph. Let  $\sigma$  be a permutation that sends  $\{i_1, \dots, i_k\}$  to itself. Narrowing then obeys:

$$(f \downarrow_{(i_1 \dots i_k)})^{(\sigma')} = (f^{(\sigma)}) \downarrow_{(i_1 \dots i_k)},$$

where  $\sigma'$  is the permutation in  $\mathbb{S}_k$  obeying:

$$\sigma'(p) = q \iff \sigma(i_p) = i_q. \quad (11)$$

If applied to a collection of node features, narrowing simply saves the features in nodes in  $i_1 \dots i_k$  and the average feature and then discards the rest. More generally, if the activation is a multi-index tensors whose indices correspond to individual nodes, narrowing forms new tensors by averaging over the nodes not in  $\{i_1 \dots i_k\}$ .

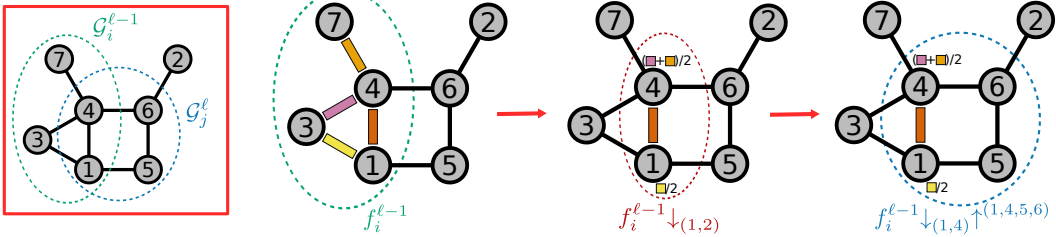


Figure 3: Example demonstrating how narrowing and promotion transfer information between local graphs. For concreteness, we assume the incoming activation  $f_i^{\ell-1}$  is a collection of edge features. We first narrow to the nodes shared between  $\mathcal{G}_i^{\ell-1}$  and  $\mathcal{G}_j^\ell$ . For the edge features used here, this corresponds to averaging over nodes 3 and 7; the edge inside the restriction is simply copied. The results are then placed into the appropriate position in the local graph of the output.

### 5.2.2 Promotion

Promotion is the opposite of narrowing in that it involves taking a function  $g: \mathbb{S}_k \rightarrow \mathbb{R}^d$  and extending it to a function on  $\mathbb{S}_m$ . We therefore apply the same construction as in Definition 1 in reverse.

**Definition 2.** Let  $(j_1, \dots, j_m)$  be an ordered set of indices with an ordered subset  $(i_1, \dots, i_k)$ . Let  $u, s, t, \bar{u}$ , and  $\bar{s}$  be as in Definition 1. Given a function  $g: \mathbb{S}_k \rightarrow \mathbb{R}^d$ , we define the **promotion** of  $g$  to  $\mathbb{S}_m$  as the function:

$$g \uparrow^{(j_1 \dots j_m)}(\tau) = \begin{cases} g(u) & \text{if } \exists u \in \mathbb{S}_k, s \in \mathbb{S}_{m-k} \text{ such that } \tau = \bar{u}st, \\ 0 & \text{otherwise.} \end{cases} \quad (12)$$

In Section 4 of the supplement we show that any such  $u$  and  $s$  are unique, and consequently our definition is independent of the representative of  $\mathbb{S}_k$  and  $\mathbb{S}_{m-k}$ . Narrowing is the pseudoinverse of promotion in the sense that for any  $g: \mathbb{S}_k \rightarrow \mathbb{R}^d$ :

$$g \uparrow^{(j_1 \dots j_m)} \downarrow_{(i_1 \dots i_k)} = g,$$

but it is not true that for any  $f: \mathbb{S}_m \rightarrow \mathbb{R}^d$ :

$$f \downarrow_{(i_1 \dots i_k)} \uparrow^{(j_1 \dots j_m)} = f,$$

since narrowing is a lossy operation. Similarly to narrowing, promotion obeys the equivariance property:

$$(g^{(\sigma')}) \uparrow^{(j_1 \dots j_m)} = (g \uparrow^{(j_1 \dots j_m)})^{(\sigma)},$$

where  $\sigma$  and  $\sigma'$  are defined as in (11). In the case of node features, promotion simply copies the node features into the new local graph. For a multi-index tensors whose indices correspond to individual nodes, promotion zero-pads the tensor, adding indices for the new nodes.

### 5.3 Autobahn neurons

Stated most generally, an Autobahn neuron  $n_j^\ell$  operates as follows. Let  $n_j^\ell$  be a neuron whose local graph  $\mathcal{G}_j^\ell$  is defined on the nodes  $\{v_{a_1}, \dots, v_{a_m}\}$ . Denote by  $f_{s_1}^{\ell-1}, \dots, f_{s_p}^{\ell-1}$  the activations of the neurons in the previous layers whose local graphs overlap with  $\mathcal{G}_j^\ell$ . We denote the nodes in the local graph of the  $z$ 'th overlapping neuron by  $(v_{a_1^z}, \dots, v_{a_{m_z}^z})$  and define the intersections:

$$\{b_1^z, \dots, b_{k_z}^z\} = \{a_1, \dots, a_m\} \cap \{a_1^z, \dots, a_{m_z}^z\}.$$

The operation performed by  $n_j^\ell$  in an Autobahn can then be summarized as follows:

- T1. Narrow each incoming activation  $f_{s_z}^{\ell-1}$  to the corresponding intersection to get  $f_{s_z}^{\ell-1} \downarrow_{(b_1^z \dots b_{k_z}^z)}$ .
- T2. Promote each of these to  $(a_1, \dots, a_m)$ :

$$\tilde{f}_z = f_{s_z}^{\ell-1} \downarrow_{(b_1^z \dots b_{k_z}^z)} \uparrow^{(a_1 \dots a_m)}.$$

Note that each  $\tilde{f}_z$  is now  $(a_1, \dots, a_m)$ -permutation equivariant.

- T3. Combine the results into a single function  $\tilde{f}$  by applying an aggregation function that is invariant to permutations of the set  $\{f_1, \dots, f_p\}$  within itself (for instance, averaging).

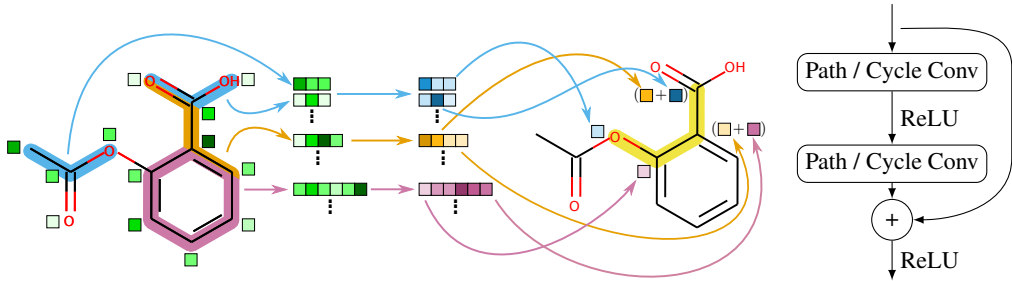


Figure 4: The internal structure of a single layer in the Autobahn architecture. We extract all path and all cycle subgraphs of fixed length and their corresponding activations. (For compactness and readability, only some activations are shown.) We then apply a series of convolutional layers. A block diagram for this step is given on the right; each isomorphism class of reference domains has its own weights. Finally, we construct the activations for the next layer by narrowing and promoting between subgraphs and summing over the resulting promoted activations.

T4. Apply one or more convolutions and nonlinearities over the local graph’s automorphism group as described in Algorithm 1.

Sufficient conditions for the resulting network to obey global permutation equivariance are given below.

**Theorem 1.** Let  $\mathbf{n}_j^\ell$  be an Autobahn neuron in a neural network operating on a graph  $\mathcal{G}$ . Let  $\mathcal{G}_j^\ell$  be the local graph of  $\mathbf{n}_j^\ell$  and denote  $\mathcal{G}_j^\ell$ ’s node set as  $\{v_{a_1}, \dots, v_{a_m}\} \subset \{v_1, \dots, v_n\}$  and its edges as  $\mathcal{E}_j^\ell = \{e_{kl}\}_{k,l \in \{v_{a_1}, \dots, v_{a_m}\}}$ . If the following three conditions hold then the resulting Autobahn obeys permutation equivariance.

1. For any permutation  $\sigma \in \mathbb{S}_n$  applied to  $\mathcal{G}$ , the resulting new network  $\Phi'$  will have a neuron  $\mathbf{n}'_{j'}$ , with the same parameters that operates on a graph  $\mathcal{G}'_{j'}$ . The nodes of  $\mathcal{G}'_{j'}$  are  $\{v_{\sigma(a_1)}, \dots, v_{\sigma(a_m)}\}$  and its edges are  $\{e_{\sigma(k)\sigma(l)} \mid e_{kl} \in \mathcal{E}_j^\ell\}$ .
2. The output of the neuron is invariant with respect to all that permutations of  $\mathcal{G}$  that leave the nodes  $\{v_{a_1}, \dots, v_{a_m}\}$  in place.
3. The output of the neuron is equivariant to all permutations of the set  $\{v_{a_1}, \dots, v_{a_m}\}$  within itself.

*Proof.* See Section 5 of the supplement.  $\square$

## 6 Molecular graphs on the Autobahn

With the Autobahn formalism defined, we return to our motivating task of learning properties of molecular graphs. From their structure of organic molecules, we see that they often have a sparse chain-like “backbone” and cyclic structures such as aromatic rings. The importance of these structures is further justified by the theory of molecular resonance. Whereas in molecular graphs edges correspond to individual pairs of electrons, real electrons cannot be completely localized to single bonds. To re-inject this physics into graph representations of molecules, chemists construct “resonance structures.” These are alternate molecular graphs formed by moving the electrons in a molecular graph inside atomic neighborhoods, often in a concerted way. Importantly, the rules of chemical valency ensure that these motions occur almost exclusively on paths or cycles within the graph. Finally, we observe that cycle and path featurizations have already been used successfully in cheminformatic applications<sup>14</sup>.

Motivated by this theory, we will choose our local graphs to correspond to cycles and paths in graph. This has the additional advantage that the one-dimensional convolution given by (6) are equivariant to the graph’s automorphism group, and can be used directly. To construct the neurons for our architecture, we extract all paths of length three through six in the graph, as well as all cycles of five or six elements. These cycle lengths were chosen because cycles of five and six elements are particularly common in chemical graphs. For each path or cycle, we construct two neurons corresponding to two ways of traversing the graph: for cycles, this corresponds to clockwise or anticlockwise rotation of the cycle, and for paths this corresponds to choosing one of the two ends to be the “initial” node.

Model	ZINC 10k (MAE, $\downarrow$ )	ZINC full (MAE, $\downarrow$ )	MolPCBA (AP $\uparrow$ )	MolHIV (ROCAUC $\uparrow$ )	MUV (AP $\uparrow$ )
GCN	$0.367 \pm 0.011$	N/A	$0.222 \pm 0.002$	$0.788 \pm 0.080$	N/A
GSN	$0.108 \pm 0.018$	N/A	N/A	$0.780 \pm 0.010$	N/A
DGN	$0.169 \pm 0.003$	N/A	N/A	<b><math>0.797 \pm 0.010</math></b>	N/A
GINE-E	$0.252 \pm 0.015$	$0.088 \pm 0.002$	$0.227 \pm 0.003$	$0.788 \pm 0.080$	0.091
HIMP	$0.151 \pm 0.006$	$0.032 \pm 0.002$	<b><math>0.274 \pm 0.003</math></b>	$0.788 \pm 0.080$	$0.114 \pm 0.041$
<b>Ours</b>	<b><math>0.106 \pm 0.004</math></b>	<b><math>0.029 \pm 0.001</math></b>	0.270	$0.780 \pm 0.003$	<b><math>0.119 \pm 0.005</math></b>

Table 1: Performance of our Autobahn architecture on two splits of the ZINC dataset and three datasets in the OGB benchmark family. compared with other recent message passing architectures. ZINC experiments use MAE (lower is better); for the metrics used in the other experiments higher is better. Baselines are other message passing architectures and were taken from [3, 7, 16] and [5].

We then construct initial features for each neuron by embedding atom and bond identities as categorical variables. Embedded atom identities are then directly assigned to the corresponding points in each path or cycle. To assign the embedded bond identities, we arbitrarily assign each bond to the preceding node in the traversals mentioned above. Since we construct a neuron for both traversal directions, this procedure does not break permutation equivariance of the architecture. Following the initial featurization, we then construct layers using the four step procedure described in Section 5. The layer is illustrated in Figure 4.

Full details of the model, including training hyper-parameters and architecture details, are available in the Supplement. The code is also freely available at <https://github.com/risilab/Autobahn>. We present empirical results from an implementation of our architecture on two subsets of the ZINC dataset using the data splits described in 16, as well as three standardized tasks from Open Graph Benchmark. All datasets are released under the MIT license. Baselines were taken from 3, 7, 16 and 5. Our automorphism-based neural network achieves state of the art results.

## 7 Conclusion

In this paper, we have introduced Automorphism-based Neural Networks, a new framework for constructing neural networks on graphs. MPNNs are specific examples of Autobahn networks constructed by choosing star-shaped templates applied to local neighborhoods. Similarly, applying Autobahn to a grid graph recovers steerable CNNs. To build an Autobahn, we first choose a collection of template graphs. We then break our input graph into a collection of local graphs, each isomorphic to a template. Computation proceeds on each local graph by applying convolutions equivariant to the template’s automorphism group, and by transferring information between the local graphs using two operators we refer to as “narrowing” and “promotion”. Our experimental results show that Autobahn networks can achieve state of the art results on several molecular learning tasks.

We expect the choice of substructure to critically influence Autobahn performance and hope to investigate this in future work. Precisely characterizing the benefits of certain substructure will require new approaches, as using automorphism group provides additional structure not found in common theoretical approaches for treating graph neural net such as the WL-hierarchy. Experimentally, we hope to explore the space of new models opened up by our theory. In learning situations where much is known about the structure, it seems clear that practitioners will be able to choose templates that correspond to known inductive biases, giving improved results. For instance, in future work we hope to improve our results on molecular graphs by adding templates that correspond to specific functional groups. For arbitrary graphs, it is not clear that the star graphs used by MPNNs are optimal or just a historical accident. It is possible that other “generic” templates exist that give reasonable results for a wide variety of graphs. For example, path activations have been used previously, in conjunction with stochastic sampling strategies, in the “Deepwalk” architecture 31. By exploring new templates, we hope to construct richer graph neural networks that more naturally reflect the graphs on which they operate.

### 7.1 Broader Impacts

In our framework, the choice of template reflects practitioner’s beliefs about which graph substructures are important for determining its properties. For social networks communities from different cultural backgrounds might result in graphs with differing topologies. Consequently, when applying Autobahn to these graphs care must be taken that chosen templates do not implicitly bias our networks towards specific cultural understandings.

## References

- [1] Emily Alsentzer, Samuel Finlayson, Michelle Li, and Marinka Zitnik. Subgraph neural networks. *Advances in Neural Information Processing Systems (NeurIPS)*, 33, 2020.
- [2] Vikraman Arvind, Frank Fuhlbrück, Johannes Köbler, and Oleg Verbitsky. On Weisfeiler-Leman invariance: Subgraph counts and related graph properties. *Journal of Computer and System Sciences*, 113:42–59, 2020.
- [3] Dominique Beaini, Saro Passaro, Vincent Létourneau, William L Hamilton, Gabriele Corso, and Pietro Liò. Directional graph networks. *arXiv preprint arXiv:2010.02863*, 2020.
- [4] Frederic E Bock, Roland C Aydin, Christian J Cyron, Norbert Huber, Surya R Kalidindi, and Benjamin Klusemann. A review of the application of machine learning and data mining approaches in continuum materials mechanics. *Frontiers in Materials*, 6:110, 2019.
- [5] Giorgos Bouritsas, Fabrizio Frasca, Stefanos Zafeiriou, and Michael M Bronstein. Improving graph neural network expressivity via subgraph isomorphism counting. *arXiv preprint arXiv:2006.09252*, 2020.
- [6] Michael M Bronstein, Joan Bruna, Yann LeCun, Arthur Szlam, and Pierre Vandergheynst. Geometric deep learning: going beyond Euclidean data. *IEEE Signal Processing Magazine*, 34(4):18–42, 2017.
- [7] Rémy Brossard, Oriel Frigo, and David Dehaene. Graph convolutions that can finally model local structure. *arXiv preprint arXiv:2011.15069*, 2020.
- [8] Zhengdao Chen, Lei Chen, Soledad Villar, and Joan Bruna. Can graph neural networks count substructures? In *Advances in Neural Information Processing Systems (NeurIPS)*, 2020.
- [9] Taco S. Cohen and Max Welling. Group equivariant convolutional networks. *Proceedings of International Conference on Machine Learning (ICML)*, 2016.
- [10] Taco S. Cohen and Max Welling. Steerable CNNs. In *International Conference on Learning Representations (ICLR)*, 2017.
- [11] Taco S. Cohen, Mario Geiger, and Maurice Weiler. A general theory of equivariant CNNs on homogeneous spaces. In *Advances in Neural Information Processing Systems (NeurIPS)*, 2019.
- [12] Pim de Haan, Taco S. Cohen, and Max Welling. Natural graph networks. In *Advances in Neural Information Processing Systems (NeurIPS)*, 2020.
- [13] Michaël Defferrard, Xavier Bresson, and Pierre Vandergheynst. Convolutional neural networks on graphs with fast localized spectral filtering. In *Advances in Neural Information Processing Systems (NeurIPS)*, 2016.
- [14] Steven L Dixon, Alexander M Smondyrev, Eric H Knoll, Shashidhar N Rao, David E Shaw, and Richard A Friesner. PHASE: a new engine for pharmacophore perception, 3D QSAR model development, and 3D database screening: 1. Methodology and preliminary results. *Journal of Computer-Aided Molecular Design*, 20(10):647–671, 2006.
- [15] David Duvenaud, Dougal Maclaurin, Jorge Aguilera-Iparraguirre, Rafael Gomez-Bombarelli, Timothy Hirzel, Alan Aspuru-Guzik, and Ryan P. Adams. Convolutional networks on graphs for learning molecular fingerprints. In *Advances in Neural Information Processing Systems (NeurIPS)*, 2015.
- [16] Matthias Fey, Jan-Gin Yuen, and Frank Weichert. Hierarchical inter-message passing for learning on molecular graphs. In *Graph Representation Learning and Beyond(GRL+) Workshop at ICML 2020*, 2020.
- [17] Vikas Garg, Stefanie Jegelka, and Tommi Jaakkola. Generalization and representational limits of graph neural networks. In *icml*, pages 3419–3430. PMLR, 2020.

[18] Justin Gilmer, Samuel S. Schoenholz, Patrick F. Riley, Oriol Vinyals, and George E. Dahl. Neural message passing for quantum chemistry. In *Proceedings of International Conference on Machine Learning (ICML)*, 2017.

[19] Mojtaba Haghatali and Johannes Hachmann. Advances of machine learning in molecular modeling and simulation. *Current Opinion in Chemical Engineering*, 23:51–57, 2019.

[20] William L Hamilton, Rex Ying, and Jure Leskovec. Inductive representation learning on large graphs. In *Advances in Neural Information Processing Systems (NeurIPS)*, pages 1025–1035, 2017.

[21] M. Henaff, J. Bruna, and Y. LeCun. Deep convolutional networks on graph-structured data. *arXiv preprint arXiv:1506.05163*, 06 2015.

[22] Weihua Hu, Bowen Liu, Joseph Gomes, Marinka Zitnik, Percy Liang, Vijay S. Pande, and Jure Leskovec. Strategies for pre-training graph neural networks. In *International Conference on Learning Representations (ICLR)*, 2020.

[23] Wengong Jin, Regina Barzilay, and Tommi Jaakkola. Junction tree variational autoencoder for molecular graph generation. In *Proceedings of International Conference on Machine Learning (ICML)*, 2018.

[24] T. N. Kipf and M. Welling. Semi-supervised classification with graph convolutional networks. In *International Conference on Learning Representations (ICLR)*, 2017.

[25] Risi Kondor and Shubhendu Trivedi. On the generalization of equivariance and convolution in neural networks to the action of compact groups. In *Proceedings of International Conference on Machine Learning (ICML)*, 2018.

[26] Alexandru Korotcov, Valery Tkachenko, Daniel P Russo, and Sean Ekins. Comparison of deep learning with multiple machine learning methods and metrics using diverse drug discovery data sets. *Molecular Pharmaceutics*, 14(12):4462–4475, 2017.

[27] Guohao Li, Matthias Müller, Ali K. Thabet, and Bernard Ghanem. DeepGCNs: Can GCNs go as deep as CNNs? In *IEEE/CVF International Conference on Computer Vision, ICCV*, 2019.

[28] Haggai Maron, Heli Ben-Hamu, Nadav Shamir, and Yaron Lipman. Invariant and equivariant graph networks. In *International Conference on Learning Representations (ICLR)*, 2018.

[29] Haggai Maron, Heli Ben-Hamu, Hadar Serviansky, and Yaron Lipman. Provably powerful graph networks. *arXiv preprint arXiv:1905.11136*, 2019.

[30] Haggai Maron, Ethan Fetaya, Nimrod Segol, and Yaron Lipman. On the universality of invariant networks. In *Proceedings of International Conference on Machine Learning (ICML)*, pages 4363–4371. PMLR, 2019.

[31] Bryan Perozzi, Rami Al-Rfou, and Steven Skiena. Deepwalk: Online learning of social representations. In *Proceedings of the 20th ACM SIGKDD International Conference on Knowledge Discovery and Data Mining*, pages 701–710, 2014.

[32] Robert Pollice, Gabriel dos Passos Gomes, Matteo Aldeghi, Riley J Hickman, Mario Krenn, Cyrille Lavigne, Michael Lindner-D’Addario, AkshatKumar Nigam, Cher Tian Ser, Zhenpeng Yao, et al. Data-driven strategies for accelerated materials design. *Accounts of Chemical Research*, 54(4):849–860, 2021.

[33] Franco Scarselli, Marco Gori, Ah Chung Tsoi, Markus Hagenbuchner, and Gabriele Monfardini. The graph neural network model. *IEEE Transactions on Neural Networks*, 20(1):61–80, 2008.

[34] Erik H. Thiede, Truong Son Hy, and Risi Kondor. The general theory of permutation equivariant neural networks and higher order graph variational encoders. *arXiv preprint arXiv:2004.03990*, 2020.

[35] Keyulu Xu, Weihua Hu, Jure Leskovec, and Stefanie Jegelka. How powerful are graph neural networks? In *International Conference on Learning Representations*, 2019.

[36] Manzil Zaheer, Satwik Kottur, Siamak Ravanbakhsh, Barnabas Poczos, Russ R Salakhutdinov, and Alexander J Smola. Deep Sets. In *Advances in Neural Information Processing Systems (NeurIPS)*, 2017.

---

# Supplementary Information for Autobahn: Automorphism-based Graph Neural Nets

---

## 1 Activations as functions on a group

In the Autobahn formalism, we make extensive use of the fact that the activations of a group-equivariant neural network can be treated as functions on the same group. Here we give a brief review for the unfamiliar reader. This formalism is also covered in detail in Sections 3 and 4 of Reference [4], although under slightly different conventions.

Consider a space  $\mathcal{X}$  acted on by a group  $G$ : at every point  $x$  in  $\mathcal{X}$ , we can apply a group element  $g \in G$ , which maps  $x$  to another point in  $\mathcal{X}$ . The action of the group on  $\mathcal{X}$  induces an action on functions of  $\mathcal{X}$ . We define an operator  $T_g$  acting on functions  $f : \mathcal{X} \rightarrow \mathbb{C}$  as follows.<sup>1</sup>

$$T_g(f)(x) = f(g(x)). \quad (1)$$

The inputs to group-equivariant neural networks are precisely functions on such spaces. For instance, for standard convolutional layers acting on images, each point on the space is a single pixel and the group of translation moves between pixels. The RGB value of each pixel is a vector-valued function of  $\mathcal{X}$ . Representations internal to the network, however, are not limited to being functions on  $\mathcal{X}$ . For instance, consider a neural network that is given a list of objects and attempts to learn an adjacency matrix. Both the list of objects and the adjacency matrix transform under permutation. Whereas each “point” in a list of objects corresponds to a single object, each “point” in the adjacency matrix corresponds to a pair of objects. While both the input and the output of the network transform according to permutation, they live on different spaces.

Fortunately, the complexity of dealing with a myriad of spaces can be avoided by mapping functions from their individual spaces to functions on  $G$ . This allows all possible spaces and group actions to be treated using a single (albeit abstract) formalism, simplifying definitions and proofs. For simplicity, we will assume that  $G$  is transitive on  $\mathcal{X}$ : for all  $x, y \in \mathcal{X}$ , there exists a group element  $g$  such that  $g(x) = y$ . (If the  $G$  is not transitive, we simply apply this procedure on every orbit of  $G$  and concatenate the results.) The construction proceeds as follows. We arbitrarily choose an initial point  $x_0$  in  $\mathcal{X}$  to act as the origin. Then, we construct the function

$$f_G(\sigma) = f(\sigma(x_0)) \quad \forall \sigma \in G. \quad (2)$$

Since we have assumed that  $G$  is transitive, this is an injective map into functions on  $G$  and preserves all of the information in  $f$ . In Figure 1, we depict this procedure, mapping the adjacency matrix for a graph with size 6 vertices to the  $S_6$ , the group of all permutations of six elements. Note that the action  $T_g$  in (1) can be extended to  $f_G$ .

$$T_g f_G(\sigma) = f(\sigma(gx_0)) = f_G(\sigma g). \quad (3)$$

## 2 Equivariance of Automorphism-based Neurons

Here, we prove that the Algorithm 1 is equivariant to permutation.

---

<sup>1</sup>Note this is a different convention for the action of group elements on functions from the one described in Reference [4]. The choice of whether to use  $T_g$  operator described here or the  $\mathbb{T}_g$  operator described in the reference is a matter of personal preference as they are inverses.

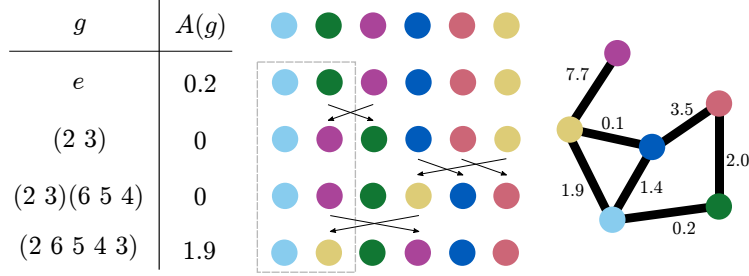


Figure 1: Example showing how function on the symmetric group can be constructed from neural network activations on the edges of a graph. We list the vertices in arbitrary order. We then construct the function as follows. For every permutation, we apply the permutation and look at two arbitrarily chosen vertices (here we have chosen the first two). If these vertices form an edge, the function takes the edge activation as its value. Otherwise, the function takes a value of zero.

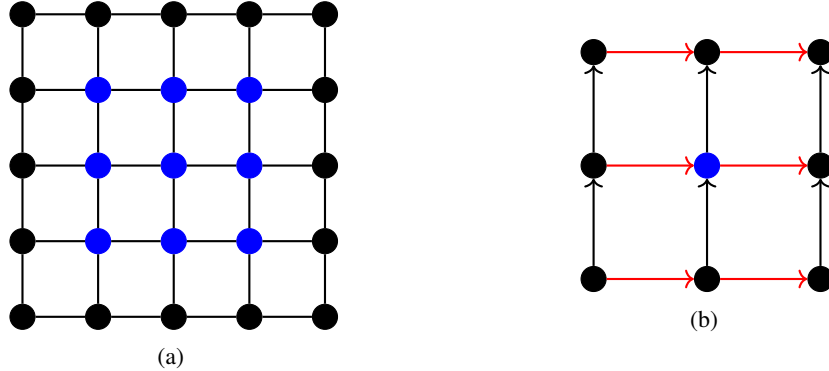


Figure 2: Template graphs for a Steerable CNN (a) and a standard convolutional neural network (b). In each case the output of the neuron is nonzero only for permutations that preserve the set of blue nodes and is invariant to permutation of the black nodes.

**Theorem 1.** Let  $\mathcal{G}$  be a graph of  $n$  vertices and let  $\sigma \in \mathbb{S}_n$ . The neuron  $\mathbf{n}^\ell$  described in Algorithm 1 obeys

$$\mathbf{n}^\ell(T_\sigma f^{\ell-1}) = T'_\sigma \mathbf{n}^\ell(f^{\ell-1}) \quad (4)$$

*Proof.* Denote the permutation of  $\mathcal{G}$  by  $\sigma$  by  $\bar{\mathcal{G}}$ . Applying  $\mathbf{n}^\ell$  to  $\bar{\mathcal{G}}$  constructs a matching  $\bar{\mu}$ . Since matching is accomplished up to an element in  $\mathcal{T}$ 's automorphism group, there exists  $v \in \text{Aut}(\mathcal{T})$  such that

$$v\mu = \bar{\mu}\sigma$$

Denoting convolution over  $\text{Aut}(\mathcal{T})$  as  $*$ , we have

$$\begin{aligned} \mathbf{n}^\ell(T_\sigma f^{\ell-1}) &= T'_{\bar{\mu}^{-1}}(\nu((T_{\bar{\mu}} T_\sigma f^{\ell-1}) * w + b)) \\ &= T'_{\bar{\mu}^{-1}}(\nu((T_v T_\mu f^{\ell-1}) * w + b)) \\ &= T'_{\bar{\mu}^{-1}} T'_v(\nu((T_\mu f^{\ell-1}) * w + b)) \\ &= T'_{\sigma^{-1}} T'_{\mu^{-1}}(\nu((T_\mu f^{\ell-1}) * w + b)). \end{aligned}$$

which proves equivariance. Note the third line follows from equivariance of convolution over  $\text{Aut}(\mathcal{T})$  and the fact that  $b$  is invariant to elements in  $\text{Aut}(\mathcal{T})$ .  $\square$

### 3 Application of Autobahn to grid graphs

Here, we discuss the application of Autobahn to grid graphs and show how the ideas in Autobahn can be used to recover the standard convolutional and steerable CNN (p4m) architectures

### 3.1 Steerable CNNs

We first recover the steerable CNN architecture for the p4m group described in Reference [1]. For concreteness, we will consider a steerable CNN constructed using a  $3 \times 3$  filter; however, the same construction can be applied to an arbitrary  $k \times k$  filter. To recover a  $3 \times 3$  steerable CNN, we will use as our template a grid of size  $5 \times 5$ . Using this larger template allows us to easily express the aggregation of all the signals in the neuron’s immediate receptive domain. Note that this resembles the use of a star graph for MPNN’s where we include both the “input” and the “output” nodes in the same template.

We first describe the output of the neuron. Each neuron outputs a function on  $\mathbb{S}_{25}$  that (a) is nonzero only for permutations that preserve the center  $4 \times 4$  nodes and (b) is constant for all permutations of the black nodes amongst each other. Furthermore, the output is nonzero only for elements corresponding to the automorphism group of the  $3 \times 3$  grid. This is the group  $D_4$  which corresponds to rotations of the grid by 90 degrees and horizontal / vertical reflections.

These outputs then form the input of the neuron in the next layer. Each neuron receives as input a function over  $D_4$  associated with each  $3 \times 3$  subgrid in Figure 2a. After narrowing and promotion, each of these function is embedded on group elements of  $\mathbb{S}_{25}$  that first send the grid to the indices  $1, \dots, 9$  and then applies the permutation corresponding to the appropriate element of  $D_4$ . Finally, each neuron applies a convolution that combines subgrid group elements of similar orientations together using a convolution over the automorphism group of the template, which is also  $D_4$ .

This example highlights the importance of having a formalism capable of more complex methods of transferring information between neurons than merely copying over node or edge features. If the input features had been sent to individual nodes and edges than we would have inadvertently averaged input signals over nodes or edges shared between incoming  $3 \times 3$  graphs.

### 3.2 Convolutional Neural Networks

As discussed in the main text, convolutional neural networks have a notion of left-right and up-down. This is information not present in a grid graph. To hope to recover a CNN from any graph neural network architecture, we must therefore consider a richer graph embedding for the image.

For a one-dimensional CNN, we can recover a CNN by considering a directed graph where edges always point in one direction. To extend this to a two-dimensional CNN, we introduce two different types of edges: “red” edges that move horizontally from pixel to pixel in the image and “black” edges that move vertically. We arbitrarily set the red edges to always point towards the right and the black edges to always point up. Then, we construct a template using the same red and black edges (depicted in Figure 2b). Each template then picks out a single  $k \times k$  subgrid in the image (again, we set  $k = 3$  for specificity in the discussion that follows). To construct each neuron, we first extend our definition of automorphism to require that automorphism must also preserve color. In this case the automorphism group of the template is the trivial group and we can take an arbitrary linear combination of all the pixels covered by our template. This is the operation performed by a standard CNN filter.

This example gives insight into the role of the automorphism group in the Autobahn formalism. In the main text the automorphism group was defined as the set of all permutations that leaves the Adjacency matrix unchanged. This choice was made simply because every graph has an adjacency matrix, ensuring that the automorphism group would be well-defined for any graph. However, if we know more about the structure of our graph, there is no reason that information cannot be included into the definition. For instance, in this example we have also required that the permutations leave a collection of edge features unchanged as well (specifically edge color). In other applications one might also further constrain the group by considering other graph attributes such as node features.

## 4 Independence of representative for promotion.

Uniqueness of  $u$  and  $s$  in the definition of promotion is a straightforward application of the following lemma.

**Lemma 2.** Let  $\tau$  and  $t$  be elements of  $\mathbb{S}_m$ . Let  $u, v \in \mathbb{S}_k$  and  $s, q \in \mathbb{S}_{m-k}$  be permutations such that

$$\tau = \dot{u}\dot{s}t = \dot{v}\dot{q}t \quad (5)$$

Then  $u = v$  and  $s = q$ .

*Proof.* It follows directly from the assumption that

$$\begin{aligned} \dot{u}\dot{s} &= \dot{v}\dot{q} \\ \implies \dot{u}\dot{s}\dot{v}^{-1}\dot{q}^{-1} &= \mathcal{I} \end{aligned}$$

Since  $\dot{v}^{-1}$  acts only on the first  $k$  elements and  $\dot{s}$  acts only on the last  $k$ , they commute and

$$\dot{u}\dot{v}^{-1}\dot{s}\dot{q}^{-1} = \mathcal{I}$$

Moreover, let  $a = uv^{-1}$  and  $b = sq^{-1}$ . It follows from the definition of  $\dot{\cdot}$  and  $\grave{\cdot}$  that

$$\grave{a} = \dot{u}\dot{v}^{-1} \text{ and } \grave{b} = \dot{s}\dot{q}^{-1}. \quad (6)$$

implying

$$\grave{a}\grave{b} = \mathcal{I}. \quad (7)$$

But this is only possible if  $a$  is the identity element of  $\mathbb{S}_k$  and  $b$  is the identity element of  $\mathbb{S}_{m-k}$ , which in turn implies  $u = v$  and  $s = q$ .  $\square$

## 5 Proof of Equivariance for Autobahn

Here, we prove that the Autobahn architecture obeys permutation equivariance. For Autobahn, neural network inputs and activations are functions on subgroups acting on a subset of the graph's vertices and global permutation of inputs can induce group operations in the associated subgroups.

Proving equivariance requires we describe how Autobahn networks transform when applying a global permutation to the input graph. To do so, we recall from Subsection 4.2 that narrowing is the pseudoinverse of promotion. Consequently, between every step in Autobahn we can promote the activation of any neuron to  $\mathbb{S}_n$  and then immediately narrow it back to the nodes in the neuron's local graph without changing the network. Doing this allows us to rewrite the steps for an Autobahn neuron  $\mathbf{n}_j^\ell$  as follows.

- T1.1 Narrow every activation  $f_{s_z}^{\ell-1}$  from  $S_n$  to  $(a_1^z, \dots, a_{m_z}^z)$ .
- T1.2 Further narrow the incoming activation  $f_{s_z}^{\ell-1}$  to the corresponding intersection to get  $f_{s_z}^{\ell-1} \downarrow_{(b_1^z \dots b_{k_z}^z)}$ .
- T1.3 Promote each  $f_{s_z}^{\ell-1} \downarrow_{(b_1^z \dots b_{k_z}^z)}$  to  $S_n$ .
- T2.1 Narrow the results back to  $(b_1^z \dots b_{k_z}^z)$ .
- T2.2 Promote each of these to  $(a_1, \dots, a_m)$ :

$$\tilde{f}_z = f_{s_z}^{\ell-1} \downarrow_{(b_1^z \dots b_{k_z}^z)} \uparrow^{(a_1 \dots a_m)}.$$

- T2.3 Promote  $\tilde{f}_z$  to  $S_n$ .
- T3.1 Narrow back down to  $(a_1, \dots, a_m)$ .
- T3.2 Apply a symmetric polynomial  $S$  to  $\tilde{f}_1, \dots, \tilde{f}_p$ :

$$\widehat{f} = S(\tilde{f}_1, \dots, \tilde{f}_p).$$

- T3.3 Promote  $\widehat{f}$  to  $S_n$ .
- T4.1 Narrow back down to  $(a_1, \dots, a_m)$ .
- T4.2 Apply one or more (learnable) equivariant linear transformations  $p_j$ , each of which is followed by a fixed pointwise nonlinearity  $\xi$ , to get the final output of the neuron.

$$f_j^\ell = \xi(p_j(\widehat{f})).$$

- T4.3 Promote every  $f_j^\ell$  to  $S_n$ .

Here, we have rewritten Autobahn so that steps T1, T2, T3, and T4 all map functions on  $\mathbb{S}_n$  to functions on  $\mathbb{S}_n$ . Consequently, we can show that each of these steps is equivariant to permutations in  $\mathbb{S}_n$ , making the network to equivariant to permutation as whole.

## 5.1 Action of permutations on narrowing and promotion

Before we prove equivariance, we first consider how a permutation of a local graphs affects the arbitrary orderings chosen when narrowing and promoting. Consider narrowing a function on  $m$  vertices onto a subset of  $k$  vertices,  $\{i_1, \dots, i_k\} \subset \{1, \dots, m\}$ . Narrowing first applies a permutation that sends the vertices indexed by  $\{i_1, \dots, i_m\}$  to the first  $k$  indices,  $(1, \dots, m)$ . Vertex  $i_1$  is sent to position 1, vertex  $i_2$  is sent to position 2, and so forth. However, this implicitly orders the vertices: If we had initially listed the vertices in a different order then they would have been sent to different positions in the set  $(1, \dots, m)$ . Consequently, when applying a permutation  $\pi$  to a local graph graph with  $m$  nodes, it is not enough to merely consider narrowing from  $\{\pi(i_1), \dots, \pi(i_m)\}$  to  $(1, \dots, m)$  as we have no guarantee of recovering the same arbitrary ordering when considering a permuted copy of the graph. Rather, we must also ensure that our network is unaffected by subsequent permutation  $p$  of the labels  $(1, \dots, m)$  caused by making a different arbitrary choice in order for the permuted graph.

Let  $f$  be an activation and  $u \in \mathbb{S}_k$ ,  $s \in \mathbb{S}_{m-k}$ , and  $t \in \mathbb{S}_m$  be permutations as in Subsection 5.2 of the main text. Upon applying a permutation  $\pi$  to a neuron's local graph, the neuron narrows the permuted activation  $T_\pi f$  to the function

$$(T_\pi f \downarrow_{(\pi(i_{p(1)}), \pi(i_{p(2)}), \dots, \pi(i_{p(k)}))}(u) = (n-k)!^{-1} \sum_{s \in \mathbb{S}_{m-k}} T_\pi f(u \circ s \circ \tau). \quad (8)$$

where  $\tau$  is an arbitrary permutation that sends  $\pi(i_1)$  to  $p(1)$ ,  $\pi(i_2)$  to  $p(2)$ , etc. Moreover, since  $t$  and  $\tau \pi$  send the same vertices to the (unordered) sets  $\{1, \dots, k\}$  and  $\{k+1, \dots, m\}$  there must exist a permutation  $a \in \mathbb{S}_{k-m}$  such that

$$p \circ a \circ t = \tau \pi. \quad (9)$$

and we can consequently write

$$\begin{aligned} T_\pi f \downarrow_{(\pi(i_{p(1)}), \pi(i_{p(2)}), \dots, \pi(i_{p(k)}))}(u) &= (n-k)!^{-1} \sum_{s \in \mathbb{S}_{m-k}} T_\pi f(u \circ s \circ \tau) \\ &= (n-k)!^{-1} \sum_{s \in \mathbb{S}_{m-k}} T_\pi f(u \circ s \circ p \circ a \circ t \pi^{-1}) \\ &= (n-k)!^{-1} \sum_{s \in \mathbb{S}_{m-k}} f(u \circ s \circ p \circ a \circ t \pi^{-1} \pi) \\ &= \sum_{s \in \mathbb{S}_{m-k}} f(u \circ p \circ s \circ a \circ t) \\ &= f \downarrow_{(\pi(i_{p(1)}), \pi(i_{p(2)}), \dots, \pi(i_{p(k)}))}(u \circ p) \\ &= T_p f \downarrow_{(\pi(i_{p(1)}), \pi(i_{p(2)}), \dots, \pi(i_{p(k)}))}(u). \end{aligned} \quad (10)$$

Similarly, promoted functions transform as

$$g \uparrow_{(\pi(i_{p(1)}), \dots, \pi(i_{p(k)}))}(\alpha) = \begin{cases} g(u) & \text{if } \exists u \in \mathbb{S}_k, s \in \mathbb{S}_{m-k} \text{ s.t. } \alpha = u \circ s \circ \tau \\ 0 & \text{otherwise.} \end{cases} \quad (11)$$

$$= \begin{cases} g(u) & \text{if } \exists u \in \mathbb{S}_k, s \in \mathbb{S}_{m-k} \text{ s.t. } \alpha = u \circ p \circ s \circ a \circ t \pi^{-1} \\ 0 & \text{otherwise.} \end{cases} \quad (12)$$

$$\implies T_p g \uparrow_{(\pi(i_{p(1)}), \dots, \pi(i_{p(k)}))} = (T_\pi g) \uparrow^{(i_1, \dots, i_k)} \quad (13)$$

## 5.2 Proof of equivariance for individual sublayers

We now prove that each of the individual sublayers T1-T4 obey equivariance.

### 5.2.1 T1 is equivariant

Since we are applying narrowing twice, we must deal with two sets of ordered vertices:  $(i_1, \dots, i_m)$  and the ordered subset to which we are narrowing,  $(j_1, \dots, j_k)$ . Throughout this section, we will

$$\begin{array}{ccccc}
(\dots, 5, 3, \dots, 2, 1, \dots, 4 \dots) & \xrightarrow[b^{-1}]{b} & (1, 2, 3, 4, 5, \dots) & \xrightarrow[t^{-1}]{t} & (2, 4, 3, \dots) \\
\rho^{-1} \uparrow \rho & & \pi^{-1} \alpha^{-1} \uparrow \pi \alpha & & \rho^{-1} \dot{\alpha}^{-1} \uparrow \rho \dot{\alpha} \\
(\dots, 4, 3, \dots, 5, \dots, 2, 4, 1) & \xleftarrow[\pi^{-1}]{\pi} & (5, 4, 1, 3, 2, \dots) & \xleftarrow[\tau^{-1}]{\tau} & (4, 2, 3, \dots, )
\end{array}$$

Figure 3: Commutative diagram depicting the permutations involved in T1 and T2. For concreteness, we have set  $k = 3$  and  $m = 5$ . Our local graph is defined on vertices vertices 1 through 5, and here we are narrowing to vertices  $j_1 = 2$ ,  $j_2 = 4$ , and  $j_3 = 2$ .

extend the  $\acute{\phantom{a}}$  and  $\grave{\phantom{a}}$  notation to both maps from  $\mathbb{S}_m$  to  $\mathbb{S}_n$  or  $\mathbb{S}_k$  to  $\mathbb{S}_n$  as necessary and trust that the precise domain and ranges of the maps will be clear from context.

Our entire graph will be acted on by a permutation  $\rho$ . We let  $b \in \mathbb{S}_n$  be an arbitrary permutation that sends the ordered set  $(i_1, \dots, i_m)$  to the first  $m$  positions and let  $\beta \in \mathbb{S}_n$  be a permutation that sends  $(\rho(i_1), \dots, \rho(i_m))$  to  $(\pi(1), \dots, \pi(m))$  for some (unknown)  $\pi$ . The permutations  $b$  and  $\beta$  play the same role as  $t$  and  $\tau$  when narrowing from  $\{1, \dots, n\}$  to  $(i_1, \dots, i_m)$ .

To aid the reader, we have summarized how global permutations affect the various subsets involved in narrowing and promotion in 3.

We now seek to prove equivariance:

$$\begin{aligned}
& \left( \left( (T_\rho f) \downarrow_{(\rho(i_{\pi(1)}), \dots, \rho(i_{\pi(m)}))} \right) \downarrow_{(\pi(j_{p(1)}), \dots, \pi(j_{p(k)}))} \right) \uparrow^{(\rho(i_{j_{p(1)}}), \dots, \rho(i_{j_{p(k)}}))} \\
&= T_\rho \left( \left( \left( f \downarrow_{(i_1, \dots, i_m)} \right) \downarrow_{(j_1, \dots, j_k)} \right) \uparrow^{(i_{j_1}, \dots, i_{j_k})} \right)
\end{aligned} \tag{14}$$

Repeatedly applying (10), we have

$$\begin{aligned}
& \left( \left( (T_\rho f) \downarrow_{(\rho(i_{\pi(1)}), \dots, \rho(i_{\pi(m)}))} \right) \downarrow_{(\pi(j_{p(1)}), \dots, \pi(j_{p(k)}))} \right) \uparrow^{(\rho(i_{j_{p(1)}}), \dots, \rho(i_{j_{p(k)}}))} \\
&= \left( \left( T_\pi \left( f \downarrow_{(i_1, \dots, i_m)} \right) \right) \downarrow_{(\pi(j_{p(1)}), \dots, \pi(j_{p(k)}))} \right) \uparrow^{(\rho(i_{j_{p(1)}}), \dots, \rho(i_{j_{p(k)}}))} \tag{15}
\end{aligned}$$

$$= \left( T_p \left( \left( f \downarrow_{(i_1, \dots, i_m)} \right) \downarrow_{(j_1, \dots, j_k)} \right) \right) \uparrow^{(\rho(i_{j_{p(1)}}), \dots, \rho(i_{j_{p(k)}}))} \tag{16}$$

$$= T_\rho \left( \left( \left( f \downarrow_{(i_1, \dots, i_m)} \right) \downarrow_{(j_1, \dots, j_k)} \right) \right) \uparrow^{(i_{j_1}, \dots, i_{j_k})} \tag{17}$$

where the last line follows by the same argument as (13).

### 5.2.2 T2 is equivariant

We seek to prove that

$$\begin{aligned}
& \left( \left( (T_\rho f) \downarrow_{(\rho(i_{j_{p-1}(1)}), \dots, \rho(i_{j_{p-1}(k)}))} \right) \uparrow^{(\pi(j_{p(1)}), \dots, \pi(j_{p(k)}))} \right) \uparrow^{(\rho(i_{(1)}), \dots, \rho(i_{(m)}))} \\
&= T_\rho \left( \left( \left( f \downarrow_{(i_{j_1}, \dots, i_{j_k})} \right) \uparrow^{(j_1, \dots, j_k)} \right) \uparrow^{(i_1, \dots, i_m)} \right)
\end{aligned} \tag{18}$$

The proof proceeds similarly to the proof for T1. We have

$$\begin{aligned}
& \left( \left( (T_\rho f) \downarrow_{(\rho(i_{j_{p(1)}), \dots, \rho(i_{j_{p(k)}))})} \right) \uparrow^{(\pi(j_{p(1)}), \dots, \pi(j_{p(k)}))} \right) \uparrow^{(\rho(i_{\pi(1)}), \dots, \rho(i_{\pi(m)}))} \\
&= \left( \left( T_p \left( f \downarrow_{(i_{j_1}, \dots, i_{j_k})} \right) \right) \uparrow^{(\pi(j_{p(1)}), \dots, \pi(j_{p(k)}))} \right) \uparrow^{(\rho(i_{\pi(1)}), \dots, \rho(i_{\pi(m)}))} \tag{19}
\end{aligned}$$

$$= \left( T_\pi \left( \left( f \downarrow_{(i_{j_1}, \dots, i_{j_k})} \right) \uparrow^{(j_1, \dots, j_k)} \right) \right) \uparrow^{(\rho(i_{\pi(1)}), \dots, \rho(i_{\pi(m)}))} \tag{20}$$

$$= T_\rho \left( \left( \left( f \downarrow_{(i_{j_1}, \dots, i_{j_k})} \right) \uparrow^{(j_1, \dots, j_k)} \right) \uparrow^{(i_1, \dots, i_m)} \right) \tag{21}$$

Modification	Validation loss
Original	$0.124 \pm 0.001$
No cycles	$0.175 \pm 0.004$
Only maximum length paths	$0.167 \pm 0.001$

Table 1: Validation loss for modified architectures on the Zinc (subset) dataset.

### 5.2.3 T3 is equivariant

To prove that applying a symmetric polynomial and applying convolution over a graph's automorphism group preserves equivariance, we require the following lemma.

**Lemma 3.** *Let  $A$  be an  $\mathbb{S}_m$  equivariant operator. Then,*

$$\left( A \left( (T_\rho f) \downarrow_{(\rho(i_{\pi(1)}), \dots, \rho(i_{\pi(k)}))} \right) \right) \uparrow^{(\rho(i_{\pi(1)}), \dots, \rho(i_{\pi(k)}))} = T_\rho f \left( \left( A \left( f \downarrow_{(i_1, \dots, i_k)} \right) \right) \uparrow^{(i_1, \dots, i_k)} \right) \quad (22)$$

*Proof.* Applying (10), the definition of equivariance, and (13) we have

$$\begin{aligned} & \left( A \left( (T_\rho f) \downarrow_{(\rho(i_{\pi(1)}), \dots, \rho(i_{\pi(k)}))} \right) \right) \uparrow^{(\rho(i_{\pi(1)}), \dots, \rho(i_{\pi(k)}))} \\ &= (A(T_\pi(f \downarrow_{i_1, \dots, i_m}))) \uparrow^{(\rho(i_{\pi(1)}), \dots, \rho(i_{\pi(k)}))} \\ &= (T_\pi(A(f \downarrow_{i_1, \dots, i_m}))) \uparrow^{(\rho(i_{\pi(1)}), \dots, \rho(i_{\pi(k)}))} \\ &= T_\rho f \left( \left( A \left( f \downarrow_{(i_1, \dots, i_k)} \right) \right) \uparrow^{(i_1, \dots, i_k)} \right) \end{aligned} \quad (23)$$

□

To prove equivariance of T3, it is therefore enough to prove that application of the symmetric polynomial is  $\mathbb{S}_m$ -equivariant. However, the output of the polynomial is invariant by definition, and it is well-known that the products are group-equivariant [3]. Consequently, the symmetric polynomials obey equivariance.

### 5.2.4 T4 is equivariant

Equivariance of T4 follows directly from Lemma 3 and the fact the neuron described by Algorithm 1 is equivariant, as shown in Section 2.

## 6 Architecture, hyper-parameter and computational details

We provide some further details into the architecture, choice of hyper-parameters and training regime of our network.

### 6.1 Architecture details

We model our block specific (i.e. cycle / path) convolutions after standard residual convolutional networks [2] with ReLU activations. We refer the reader to our pytorch implementation for details of the implementation.

We perform a simple ablation study of the main components of the model on the Zinc-subset problem. In particular, we study the impact of omitting: i) the cycle-based convolutions and ii) the paths shorter than the maximum length considered. Validation loss<sup>2</sup> results are reported in table 1.

<sup>2</sup>Note that for this particular dataset, validation losses tend to be higher than test losses, which is also observed in some other architectures such as HIMP.

Dataset	Channels	Dropout	Epochs	Warmup	Decay milestones
Zinc (subset)	128	0.0	600	15	150, 300
Zinc	128	0.0	150	5	40, 80
MolPCBA	128	0.0	50	5	35
MolHIV	128	0.5	60	15	N/A
MolMUV	64	0.0	30	5	N/A

Table 2: Hyper-parameter and training schedules used on each dataset.

Path length	Validation Loss	Training Time
4	$0.140 \pm 0.000$	3 h15 min
5	$0.135 \pm 0.000$	4 h50 min
6	$0.124 \pm 0.000$	6 h50 min
7	$0.121 \pm 0.001$	9 h30 min

Table 3: Performance and training time of model on Zinc (subset) as a function of maximum path length considered.

## 6.2 Hyper-parameter details

Our hyper-parameters were chosen based on a combination of chemical intuition and cursory data-based selection, with some consideration towards computational cost. As our architecture specification is quite general, the number of hyper-parameters is potentially large. In practice, we have restricted ourselves to tuning three parameters: a global network width parameter (which controls the number of channels in all convolutional and linear layers), a dropout parameter (which controls whether dropout is used and the amount of dropout), and the training schedule. The values used are specified in table 2. The training schedule is set with a base learning rate of 0.0003 at batch size 128 (and scaled linearly with batch size). The learning rate is increased linearly from zero to the base rate during the specified number of warmup epochs, and is then piecewise-constant, with the value decaying by a factor of 10 after each milestone.

The lengths of the paths and cycles considered in the model are also hyper-parameters of the model. We used the same values (cycles of lengths 5 and 6, and paths of lengths 3 to 6 inclusive) in all of our models. We note that in molecular graphs, cycles of lengths other than 5 and 6 are exceedingly rare (e.g. in the Zinc dataset, cycles of lengths different from 5 or 6 appear in about 1% of the molecules). We evaluate different possibilities for the maximum length of paths to be considered in table 3, we observe that in general, both computational time and prediction performance increase with larger path lengths.

## 6.3 Computational details

In a message passing graph neural network, computational time is typically proportional to the number of edges present in the graph. On the other hand, our Autobahn network scales with the number of paths and cycles present in the graph. An immediate concern may be that the number of such structures could be combinatorially large in the size of the graph. In table 4, we show that, due to their tree-like structure, molecular graphs do not display such combinatorial explosion of number of sub-structures in practice.

The computational cost of our model scales roughly linearly with the total number of substructures under consideration. In practice, for molecular graphs, selecting only paths of short lengths and cycles, we expect the computational cost to be on the same order of magnitude as standard graph neural networks. We report the total amount of time (in GPU-hours) required for training each of our model in table 5. The training was performed on Nvidia V100 GPUs, and mixed-precision computation was used for all models except MolHIV were some gradient stability issue were encountered. The two largest datasets (Zinc an MolPCBA) were trained on four GPUs, whereas the remaining datasets were trained on a single GPU.

Dataset	Nodes	Edges	Paths						Cycles	
			3	4	5	6	7	8	5	6
Zinc	23.1	49.8	34.6	43.9	55.0	64.4	65.8	70.2	0.56	1.70
MolPCBA	26.0	56.3	39.3	51.0	65.2	79.5	84.2	93.1	0.50	2.23
MolHIV	25.5	54.9	39.2	52.1	68.9	87.2	97.2	111.5	0.34	2.01
MolMUV	24.2	52.5	36.5	47.6	61.1	73.4	77.2	84.6	0.63	2.02

Table 4: Average count of structures in various datasets.

Dataset	Samples	Samples / s / GPU	Training time (GPU-hours)
Zinc (subset)	6.0M	280	6.8 h
Zinc	33.0M	215	42.7 h
MolPCBA	21.9M	171	35.5 h
MolHIV	2.5M	114	6.1 h
MolMUV	2.8M	222	3.5 h

Table 5: Computational cost of training provided models. Samples denotes total number of gradients computed (i.e. number of epochs times number of observations in dataset).

## References

- [1] Taco S. Cohen and Max Welling. Steerable CNNs. In *International Conference on Learning Representations (ICLR)*, 2017.
- [2] Kaiming He, Xiangyu Zhang, Shaoqing Ren, and Jian Sun. Deep residual learning for image recognition. In *Proceedings of the IEEE conference on computer vision and pattern recognition*, pages 770–778, 2016.
- [3] R. Kondor, Z. Lin, and S. Trivedi. Clebsch–Gordan nets: a fully Fourier space spherical convolutional neural network. *ArXiv e-prints*, 1806.09231, June 2018.
- [4] Risi Kondor and Shubhendu Trivedi. On the generalization of equivariance and convolution in neural networks to the action of compact groups. In *Proceedings of International Conference on Machine Learning (ICML)*, 2018.